Optics and Spectroscopy, 2023, Vol. 131, No. 1

20

Spectral methods for study of the G-protein-coupled receptor rhodopsin. III. Osmotic stress effects

© A.V. Struts[1,2,3], A.V. Barmasov[1,2], M.F. Brown[3]

[1] St.-Petersburg State Pediatric Medical University,
194100 St.-Petersburg, Russia
[2] St.-Petersburg State University,
199034 St.-Petersburg, Russia
[3] University of Arizona,
Tucson, AZ 85721 USA
e-mail: struts@arizona.edu

Received October 28, 2022
Revised January 6, 2023
Accepted January 9, 2023

We review osmotic stress studies of the G-protein-coupled receptor rhodopsin. Despite the established presence of small amounts of structural water in these receptors, the influence of bulk water on their function remains unknown. Investigations of osmotic stress effects on the GPCR archetype rhodopsin have provided unique data about the role of water in receptor activation. It was discovered that osmolytes shift the rhodopsin equilibrium after photoactivation, either to the active or inactive conformations depending on their molar mass. Experimentally at least 80 water molecules have been found to enter rhodopsin in the transition to the active state. We propose that this influx of water is a necessary condition for receptor activation. If the water movement is blocked, e.g., by large osmolytes or by dehydration, then the receptor does not undergo its functional transition. The results suggest a new model whereby rhodopsin becomes swollen and partially unfolded in the activation mechanism. Water thus acts as a powerful allosteric modulator of functioning for rhodopsin-like receptors.

Keywords: G-protein-coupled receptors, membranes, optical spectroscopy, rhodopsin, signal transduction.

DOI: 10.21883/EOS.2023.01.55528.4261-22

Introduction

The current paper continues our review of spectral studies of rhodopsin [1,2]. Here we focus on osmotic stress effects. G-protein-coupled receptors (GPCRs) are integral membrane proteins involved in the regulation of multiple biological processes in vertebrates by transmitting signals across cellular membranes. Somewhere between 30 to 50% of drugs target diseases related to dysfunction of pathways of rhodopsin-like receptors [3–6]. Dozens of GPCR structures have become available in recent years due to essential progress in their crystallization [7–9]. Although X-ray analysis has provided a great volume of structural information including active states, the specific experimental conditions (low temperatures, dehydration, and the absence of membrane environment) do not allow one to obtain the whole picture of GPCR functioning. Recent investigations of rhodopsin by small-angle and quasielastic neutron scattering indicate swelling of the receptor due to water absorption upon activation [10,11], a conclusion that is also supported by molecular dynamics (MD) simulations [12,13]. Moreover, wide-angle X-ray scattering (WAXS) studies [14] indicate that at room temperature the structural changes of rhodopsin due to activation may be larger than revealed earlier by X-ray crystallography. In this respect, quantitative data are needed on the rhodopsin volume change in the active state. Here we review osmotic stress studies of rhodopsin, which are ideally suited to estimate the amount of water absorbed by the receptor in its activation mechanism. Furthermore, we discuss the role of water in this process, which surprisingly turns out to be much more important than just providing a medium for organizing the cellular components.

Estimation of hydration changes in rhodopsin upon activation

Rhodopsin activation occurs after absorption of a photon by 11-*cis* retinal and its isomerization to the all-*trans* conformation. The general reaction scheme for rhodopsin activation can be described by the following time-ordered sequence [15–18]:

$$\mathrm{Rh}\ + h\nu \rightarrow \mathrm{MI} \rightleftharpoons \mathrm{MII}_a \rightleftharpoons \mathrm{MII}_b + \mathrm{H_3O^+} \rightleftharpoons \mathrm{MII}_b\mathrm{H}^+,$$

where Rh is dark-state rhodopsin with 11-*cis* retinal covalently bound to rhodopsin by a protonated Schiff base linkage, MI is the preactive state with all-*trans* retinal and protonated Schiff base, MII_a is the state with a deprotonated Schiff base yet is in the inactive conformation, MII_b is the active state, and $\mathrm{MII}_b\mathrm{H}^+$ is the active state additionally stabilized with the Glu^{134} residue protonated. It should be noted that the last four states populate an energy landscape and are in dynamic equilibrium after photoactivation, which can be shifted by changing the environmental conditions (pH, temperature, or membrane composition) [17,19–21]. Structurally the MII_b states are characterized by rotation of the cytoplasmic end of transmembrane helix 6 (TM6) away from the rest of the helical bundle that opens the binding cleft for the G-protein transducin (Gt). This activating motion of the helix 6 together with elongation of helix 5 suggests an increase of the receptor volume and greater internal hydration [7,11,18,22,23].

Application of the osmotic stress protocol has been used to measure changes in the number of water molecules associated with functional activity of soluble enzymes such as hemoglobin [24], hexokinase [25], adenosine deaminase [26], as well as membrane proteins: potassium channels [27], alamecithin [28], sodium channels [29], and cytochrome c oxidase [30]. In the case of membrane proteins, one should also account for the interaction of water with the membrane lipids. Changes in water activity govern phospholipid acyl chain packing [31], bilayer thickness [32,33], curvature [20], and the lateral diffusion coefficient of phospholipids [34].

Previously the effect of hydration on rhodopsin activation and on acyl chain packing in the rod outer segment (ROS) disk membranes has been studied with glycerol, sucrose, and stachyose osmolytes [35], Fig 1. The equilibrium constant for the transition from the inactive MI to the active MII state, $K_{\text{eq}} = [\text{MII}]/[\text{MI}]$, was calculated from the electronic (UV/visible) absorption bands of MI and MII, Fig. 1, *a*. The insert in Fig. 1, *a* shows the electronic absorption spectra of rhodopsin in disk membranes before and after bleaching [36]. First, the difference spectra (4)−(1), (3)−(1), and (4)−(3) corresponding to 100% content of rhodopsin and retinal oxime, $f_1 = 1$, unbleached, f_2, and bleached, f_3, fractions were modeled using the following function [36]:

$$\begin{aligned} A(\lambda)_n = {} & f_n A_{\text{ox}} \Big\{ \exp\big(-\big[(|1/\lambda - 1/\lambda_{\text{ox}}|/W_{\text{ox,l}})^{P_{\text{ox,l}}}\big]\big) \\ & + \exp\big(-\big[(|1/\lambda - 1/\lambda_{\text{ox}}|/W_{\text{ox,h}})^{P_{\text{ox,h}}}\big]\big) \Big\} \\ & - f_n A_{\text{rho}} \Big\{ \exp\big(-\big[(|1/\lambda - 1/\lambda_{\text{rho}}|/W_{\text{rho,l}})^{P_{\text{rho,l}}}\big]\big) \\ & + \exp\big(-\big[(|1/\lambda - 1/\lambda_{\text{rho}}|/W_{\text{rho,h}})^{P_{\text{rho,h}}}\big]\big) \Big\}. \end{aligned} \tag{1}$$

Here A_i is the absorbance of species i at its wavelength of maximum absorbance, λ_i, and $W_{i,j}$ and $P_{i,j}$ characterize the width and power dependence of species i at wavelengths lower (j = l) and higher (j = h) than its peak maximum, respectively. After determination of the parameters of the rhodopsin and retinal oxime (ox) absorbance profiles, the contributions of these components were subtracted from the (2)−(1), (2)−(3), and (2)−(4) difference spectra. The resulting three spectra were almost identical to each other and contained only the MI and MII absorbance profiles. A function analogous to Eq. (1) was then used to determine the parameters A_i, λ_i, $W_{i,j}$, and $P_{i,j}$ characteristic of MI and MII by globally fitting the three corrected difference spectra. These spectra were then averaged to produce the final deconvoluted MI–MII equilibrium spectrum, Fig. 1, *a* [36]. The change in the number of water molecules associated with the protein upon activation, ΔN_{w}, is given by the slope of the $\ln K_{\text{eq}}$ value versus the osmolyte concentration [37], Fig. 1, *b*:

$$\ln K_{\text{eq}} = -\Delta N_{\text{w}} \frac{[\text{osmolal}]}{55.6}. \tag{2}$$

The osmolality of solutions [osmolal] is determined with a vapor pressure osmometer.

In previous research [35], analysis of the fluorescence anisotropy decay of 1,6-diphenyl-1,3,5-hexatriene (DPH) in terms of the rotational diffusion model has revealed that the angular width of the orientational distribution of DPH about the membrane normal was narrowed with increased osmolality. The orientational freedom of DPH is characterized by the parameter f_{v} [38], Fig. 1, *c*, which is defined by

$$f_{\text{v}} = \frac{1}{2f(\theta)_{\max}}. \tag{3}$$

The angular distribution function $f(\theta)$, Fig. 1, *c* is given by

$$f(\theta) = N^{-1} \exp\big[\lambda_2 P_2(\cos\theta) + \lambda_4 P_4(\cos\theta)\big],$$

where $P_2(\cos\theta)$ and $P_4(\cos\theta)$ are the 2nd and 4th Legendre polynomials, and N is the normalization constant. The $\ln K_{\text{eq}}$ and f_{v} concentration dependences show that the solution osmolality increases the equilibrium concentration of MII and simultaneously increases the acyl chain packing in membranes, which contradicts previously reported observations [39].

According to Fig. 1, *b*, the shift of the metarhodopsin equilibrium to the active MII state by osmolytes means that this state is less hydrated, according to Le Châtelier's principle. It was estimated that 20 water molecules are released during the MI-to-MII transition at 20°C, and that 13 waters are released at 35°C [35]. Note that X-ray crystallographic studies are not sensitive to the bulk water movement upon receptor activation and reveal only a few structural water molecules present in the dark and the active states of rhodopsin. By contrast MD simulations [12] have indicated an oposite influx of about 80 water molecules into rhodopsin associated with its activating helical motion. Also, neutron scattering studies showed that rhodopsin hydration and the radius of gyration increase in the activation process [10,11]. Therefore, the question arises: is the active MII state more or less hydrated versus the inactive dark state?

Is the preactive MI or active MII state more hydrated?

To resolve this controversy, the effect of hydration on rhodopsin activation was studied using a series of hydrophilic polymer osmolytes with different molar

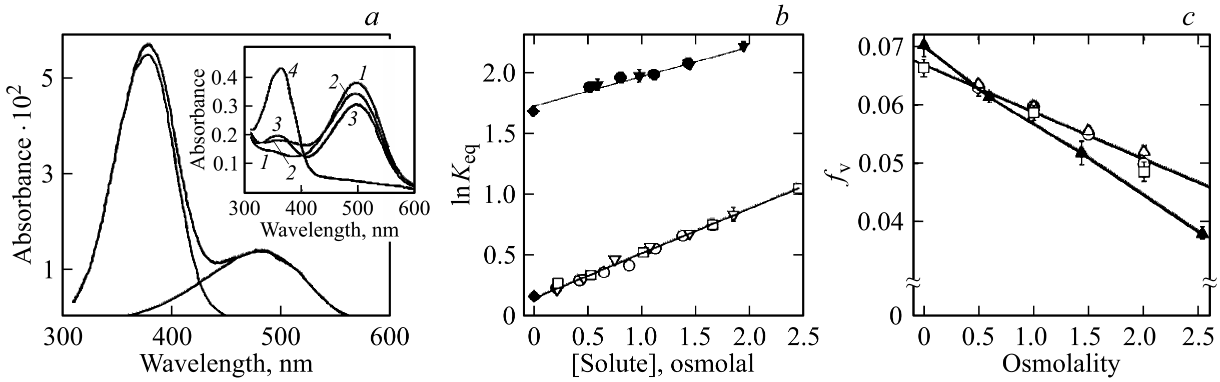

Figure 1. (*a*) An example of deconvoluted difference spectra for MI–MII rhodopsin equilibrium in mildly sonicated retinal disk membranes at pH 7.0 and $T = 30°C$ with individual MI (right) and MII (left) spectra. Insert shows the absorbance spectra of rhodopsin from which the above deconvoluted spectra were derived. Spectra were measured first before bleaching (1), after partial bleaching (2), following addition of hydroxylamine (3), and after complete bleaching in the presence of hydroxylamine (4). (*b*) Effects of solute osmolality on equilibrium constant K_{eq} for the MI–MII equilibrium at $T = 20$ and 35°C. The slope of each line equals $-\Delta N_w/55.6$, where ΔN_w is the change in the number of water molecules in solute-inaccessible regions of the protein. (○) Glycerol, 20°C; (▽) sucrose, 20°C; (□) stachyose, 20°C; (●) glycerol, 35°C; and (▼) sucrose, 35°C; (♦) control, both temperatures. (*c*) Effect of solute osmolality on the parameter f_v at $T = 20$ and 35°C. (O) Glycerol, 20°C; (△) sucrose, 20°C; (□) stachyose, 20°C; and (▲) sucrose, 35°C. Figure is adapted from Refs. [35,36].

masses [40], Fig. 2. Water-soluble polymers (polyethylene glycol, PEG) were chosen to control the rhodopsin hydration because of the relatively high osmotic pressures (Π) that can be achieved (> 10 MPa). The fraction of the active MII state was monitored by UV/visible spectroscopy, Fig. 2, *a*. Difference spectra of rhodopsin (bleached minus dark states) in disk membranes, Fig. 2, *a*, were simulated as a linear combination of the basis difference spectra of the MI, $\Delta A_{MI}(\lambda)$, and MII, $\Delta A_{MII}(\lambda)$, states measured at pH 9.5 and 10°C or pH 5 and 21°C correspondingly: $\Delta A(\lambda) = (1-\theta)\Delta A_{MI}(\lambda) + \theta\Delta A_{MII}(\lambda)$. The fraction of the MII state, θ, was used as a fitting parameter and was determined from fitting to the experimental difference spectrum. Alternatively, θ was calculated from the crossover point, λ_0, of the difference spectrum of the bleached sample: $\theta = (\lambda_0 - \lambda_{MI})/(\lambda_{MII} - \lambda_{MI})$, where λ_{MI} and λ_{MII} are the crossover points of the basis difference spectra [40,41]. The pH titration curves for rhodopsin directly show how the polymer osmolytes reversibly shift the metarhodopsin equilibrium to either the inactive (closed) MI state or the active (open) MII state, Fig. 2, *b, c*. For a protein like rhodopsin, by the Law of Mass Action, the back shifting of the activation equilibrium to the inactive MI state means that in the forward direction (transition from MI to MII state) an influx (flood) of water occurs. The nearly linear isotherms for different osmolytes ($\ln K_{eq}$ versus Π), Fig. 2, *c*, reveal a negative slope for large molar mass (M_r) osmolytes (PEG 1500 and PEG 400), yet a positive slope for small osmolytes (PEG 300 and PEG 200). Thus, osmolytes with a large molar mass favor the inactive MI state (closed conformation). Small osmolytes, on the other hand, increase the active (open) MII fraction in agreement with previous work [35]. However, because the withdrawal of water by large osmolytes and the shift of the equilibrium to the inactive MI state is observed, we conclude that the active MII state is more hydrated.

Furthermore, we propose that the opposite conclusion of the previous paper [35] is based on usage of relatively small osmolytes, which penetrate the transducin (G-protein) binding cavity and cannot completely withdraw water from the receptor. For the same reason, the number of water molecules which enter the receptor upon activation should be calculated for the largest osmolytes, that are entirely excluded from the rhodopsin. The equilibrium constant ($K =$[MII]/[MI]) depends on osmotic pressure Π according to

$$\left(\frac{\partial \ln K}{\partial \Pi}\right)_T = -\frac{\Delta V^\circ}{RT}, \qquad (4)$$

where $\Delta V^\circ \approx N_w \bar{V}_w$ is the standard change in excess (partial) water volume of the initial and final states, the number of water molecules is N_w, and $\bar{V}_w$ is the water partial molar volume. In this way, we estimate the influx of water upon light activation as approximately 80 water molecules as a lower limit. For partially excluded polymers (PEG 400), the apparent volume change is given by $V_{app} = \Delta V^\circ(1-P)$, in terms of the partition coefficient P between the solution and the protein. That means a reduction of the apparent rhodopsin hydrated volume occurs upon activation in the presence of small osmolytes. However, negative ΔV_{app} values are observed for small osmolytes (sucrose, PEG 200), Fig. 2, *e*. Evidently, the negative apparent hydrated volume is not related to real influx or withdrawal of water but to shifting of the metarhodopsin equilibrium to the active MII state because of other interactions.

One possible explanation is that this trend is due to the interaction of small osmolytes with lipids, since osmotic

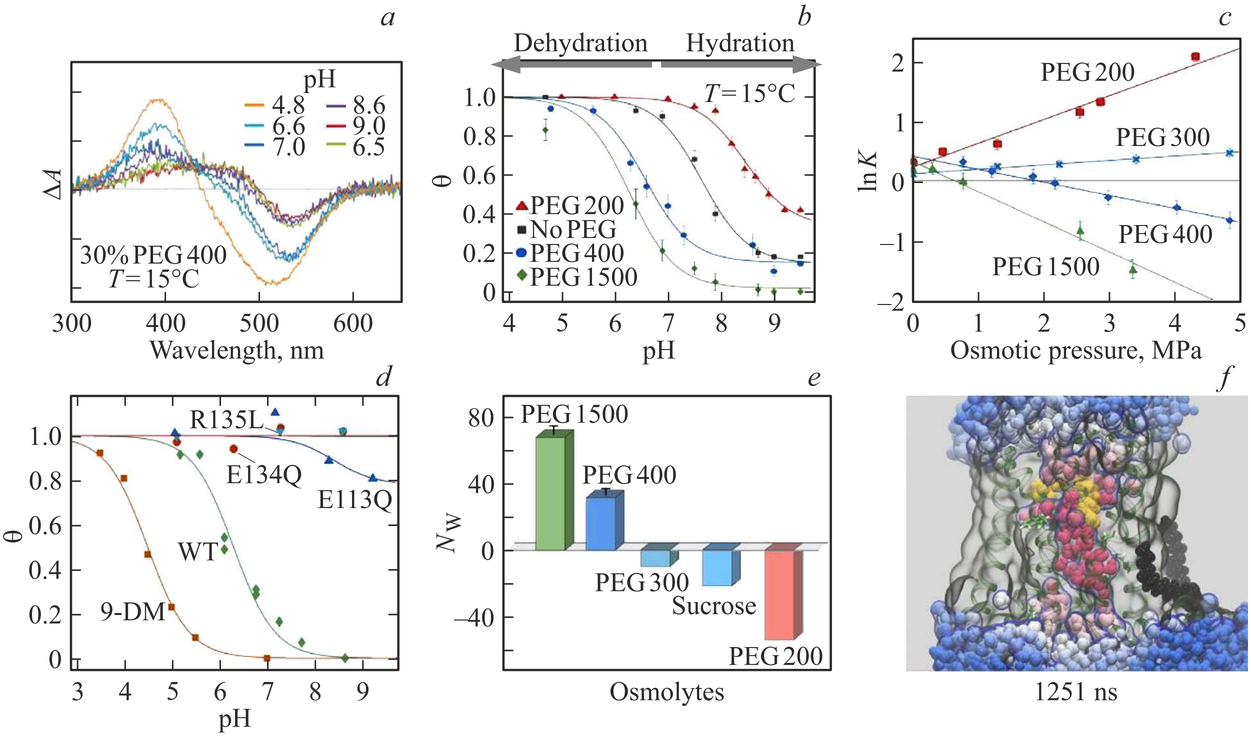

Figure 2. (*a*) Representative electronic UV/visible difference absorption spectra of rhodopsin (photobleached minus dark state). (*b*) Fraction of active MII state (θ) versus pH showing effect of controlled hydration ($T = 15^\circ$C) for osmolytes of different molar mass (M_r) (30–35% w/w polyethylene glycol, PEG). (*c*) Metarhodopsin (MII/MI) ratio ($\ln K$) plotted versus osmotic pressure (Π) for different size PEG osmolytes (pH 7.4, $T = 15^\circ$C). (*d*) Active MII fraction (θ) versus pH comparing wild-type (WT) rhodopsin in RDM ($T = 0^\circ$C) to constitutive mutants in egg phosphatidylcholine (PC) membranes ($T = 10^\circ$C) and to WT rhodopsin with retinoid antagonists (9-desmethylretinal, 9-DM) in RDM ($T = 20^\circ$C) [42-44]. (*e*) Apparent number (N_W) of water molecules taken up or released from light-activated rhodopsin for polymer (PEG) osmolytes and sucrose. (*f*) Snapshot of molecular dynamics (MD) simulation of rhodopsin 1.25 ms after retinal isomerization in silico [12]. Internal water molecules (red) flood the transducing binding cleft forming a channel to the retinal ligand. Figure is from Ref. [40].

interaction with the protein is reduced by the partial or complete osmolyte penetration into the transducin binding cavity. In that case, membrane dehydration increases the bilayer thickness as demonstrated by solid-state ^{2}H NMR spectroscopy [32,33]. Dehydration can also lead to greater magnitude of the negative monolayer spontaneous curvature, as described by the flexible surface model (FSM) [20]. Both effects will promote active MII formation in lipid bilayers [20,45,46]. Moreover, experimental site-directed spin labeling (SDSL) studies [47] of rhodopsin in *n*-Dodecyl-β-D-maltoside (DDM) micelles have shown that the small osmolyte sucrose back shifts the population toward the MI component. Because the forward shifting to MII is absent in the detergent-solubilized system, a role of the lipid bilayer is supported in favoring the active state in the presence of small osmolytes. On the other hand, increased order parameters for lipid segmental motion in the case of increased thickness of the membrane bilayer may indicate decreased flexibility of lipids and that generally inhibits rhodopsin activation. Consequently, the lipid influences may be complex, and the resulting effect requires further investigation. Other factors should be considered for small osmolytes as well.

Partial penetration of small osmolytes into the protein might also withdraw water from smaller internal cavities associated with the MI–MII transition [6,7,48,49]. One example is offered by recent direct hydration experiments monitoring bound water by infrared spectroscopy in opsin and the E134Q mutant, suggesting that Glu^{134} of the conserved E(D)RY motif is a hydration site at the protein-lipid interface, which dehydrates going from MII$_b$ to the MII$_b$H$^+$ state [50]. Local dehydration of small protein regions such as these is consistent with MII stabilization by small osmolytes [35] (see Fig. 1, *b*, 2, *b, c*). The shift to the MII state could also be attributed to specific interaction of small osmolytes with the transducin binding cavity. Specific PEG-protein interactions are known to be inversely related to PEG size [51]. Still, we did not observe any substantial binding of small osmolytes to rhodopsin (see below).

Mutagenesis is often used to investigate the role of various functional groups in protein activation. To address the effect of constitutive mutations, Fig. 2, *d* shows titration curves for the E113Q, R135L, and E134Q mutants that

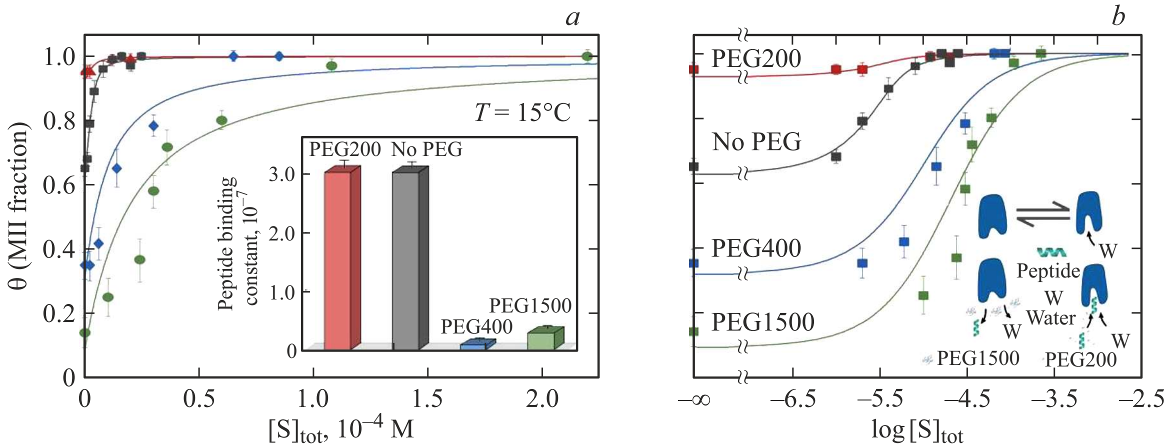

Figure 3. (a) Active MII fraction (θ) in native retinal disk membranes (RDM) versus total concentration ($[S]_{tot}$) of high-affinity transducin C-terminal peptide analogue (pH 7.4, $T = 15^\circ$C). Data are fit to a single-site binding isotherm. Inset: effect on peptide binding constant for different size polymer osmolytes. (b) Active MII fraction (θ) versus $\log [S]_{tot}$ value. Inset: Illustration of how C-terminal peptide competes with large osmolytes (PEG 1500) yet is noncompetitive for small osmolytes (PEG 200). Figure is from Ref. [40].

stabilize the active state of the receptors. In addition, we show results for rhodopsin regenerated with a retinal analog lacking the methyl group at position C9 (9-desmethylretinal, 9-DM) [42–44] which favors the inactive state. Obviously, the effect of the E113Q, R135L, and E134Q mutations is similar to the influence of small osmolytes, while substitution of the 11-*cis* retinal with 9-desmethylretinal results in the shift of rhodopsin equilibrium to the inactive state, analogous to the effect of large osmolytes. However, what are the mechanisms for the influences of these so different factors? The effect of E113Q, R135L, and E134Q mutations is associated with the disruption of the first (in the case of E113Q) and second (in the case of R135L and E134Q) ionic locks that stabilize the inactive conformation of rhodopsin due to the neutralization of residues Glu^{113}, Asp^{135}, and Glu^{134}. On the other hand, 9-DM retinal, due to the absence of a methyl group, is apparently unable to maintain the position and orientation of the β-ionone ring between helices 5 and 6, necessary for the activating rotation of helix 6. The action of osmolytes is mainly based on osmotic interaction with the transducin binding cavity in rhodopsin. We also note that the effect of pH on the shift of the equilibrium between MI and MII is associated with the protonation of Glu^{134}, while the effect of temperature change is associated with a change in the contribution of entropy to the free energy of photoactivated rhodopsin. However, in the end, the influence of all factors is reduced to a change in the free energy of the photoproduct.

Effect of hydration on G-protein binding

Next, it was established that increased hydration drives binding of the C-terminal α-helix of the cognate G-protein to rhodopsin, while dehydration causes its unbinding [40]. Figure 3 shows the dependence of the active MII fraction in the native retinal disk membrane (RDM) on concentration of the transducin C-terminal peptide analogue (amino acid sequence ILENLKDVGLF) in the presence of different osmolytes. This peptide has high binding affinity to rhodopsin and stabilizes the active MII state when bound to the receptor. Fitting the binding isotherms, Fig. 3, *a, b*, indicates that larger polymers (PEG 1500 and PEG 400) decrease the binding affinity by an order of magnitude. That means the interaction of large osmolytes and the transducin peptide with the protein is competitive. For smaller osmolytes ($M_r < 400$ Da), the effect is absent (inset of Fig. 3, *a*). Thus, small osmolytes do not compete for binding to rhodopsin with the transducin peptide, and consequently they do not bind to the protein. Detailed analysis shows that for large osmolytes, the peptide binding constant correlates with proton uptake by Glu^{134} of the conserved E(D)RY sequence motif. Hence, water not only governs the equilibrium between active and inactive states [52] of the receptor, but also affects the intrinsic binding of its cognate G-protein.

Extended osmotic stress studies

Further osmotic stress studies were performed for an extended range of pH values, osmolyte concentrations, and molecular weights. Fig. 4 shows that influences of pH on rhodopsin activation in the pH range from 3 to 10 can be described by a phenomenological Henderson-Hasselbalch equation involving two pK_A values and an alkaline endpoint. The rhodopsin states are distinguished by having a protonated or deprotonated Schiff base (PSB or SB, indicated by a subscript), while a superscript indicates the charge relative to MI, Fig. 4, *a*. The lower pK_A (designated „Schiff base pK_A") reflects the pH-dependent protonation of the retinal Schiff base, which lowers the

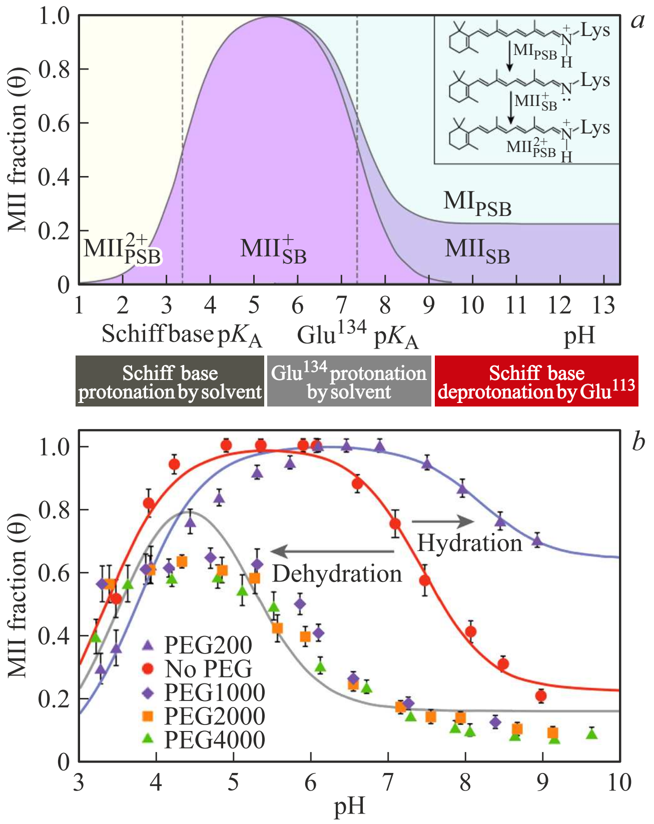

Figure 4. (a) Influences of pH on rhodopsin activation. The lower pK_A (Schiff base pK_A) reflects protonation of the retinal Schiff base. The higher pK_A value (Glu^{134} pK_A) reflects protonation of Glu^{134} which stabilizes the fully active MII state. (b) Osmotic stress from large osmolytes (50% wt/wt at $T = 15^\circ C$) back shifts the apparent Glu^{134} pK_A value from 7.4 to 5.2. At 30% wt/wt PEG 200 ($T = 15^\circ C$) the Glu^{134} pK_A is maximally forward shifted to 8.2 favoring the active MII state. Figure is from Ref. [41].

apparent MII fraction detected by UV/visible spectroscopy. The higher pK_A value (designated „Glu^{134} pK_A“) indicates protonation of Glu^{134} in the E(D)RY motif to stabilize the fully active MII conformation. The alkaline endpoint at higher pH corresponds to MII substates that persist at higher temperatures even when Glu^{134} is fully deprotonated. Small osmolytes stabilize the open MII conformation by shifting the pK_A to the alkaline region and by increasing the alkaline endpoint, Fig. 4, b. By contrast, dehydrating large osmolytes decrease the deprotonated MII population by shifting the pK_A to the acidic region and by lowering the alkaline endpoint.

Furthermore, increased range of osmolyte concentrations and molecular weights revealed apparent compressibility effects for large osmolytes and saturation effects for small osmolytes. Fig. 5, a indicates that the dependence of $\ln K$ and correspondingly the molar hydration volume on osmotic pressure is not linear, so that the second-order term needs to be considered in the virial expansion of $\ln K$ in terms of osmotic pressure:

$$\ln K = \ln K^\circ - \left(\frac{\Delta V^\circ}{RT}\right)\Pi + \left(\frac{1}{2}\Delta C\right)\Pi^2. \qquad (5)$$

Fitting the data with this quadratic function yields the change in protein hydrating volume ΔV° between MI and MII and the number of hydrating water molecules per mole of rhodopsin N_w under standard-state (zero osmotic pressure) conditions. Using the relation $\Delta V^\circ \approx N_w \bar{V}_w$ for the MI–MII transition, where $\bar{V}_w$ is the partial molar volume of water, for large PEG osmolytes with molar mass between 1000 and 6000 Da, an increase of 80 to 100 water molecules was calculated for the MI–MII transition. The second virial coefficient changes ΔC on the order of $0.1\,MPa^{-2}$, and seems to correspond to changes in osmotic compressibility of $\sim 0.01\,MPa^{-1}$.

On the other hand, small molar mass osmolytes (PEG 200–PEG 600) affect rhodopsin differently: at small concentrations they forward shift $\ln K_{eq}$ to the MII state. However, a saturation effect is observed at higher concentrations beyond which the equilibrium is back shifted to MI resembling the large osmolyte behavior. As PEG size increases, the range for the forward shifting to MII diminishes. We already discussed how small osmolytes may shift the metarhodopsin equilibrium to the active state. As for the saturation effect, obviously at small osmolyte concentrations they penetrate the transducing binding cavity without limitations. Nevetherless, when the concentration increases, they cannot have the same spatial distribution inside and outside the binding cavity due to its (cavity) limited size. Hence the external concentration becomes larger than the internal one, and they start to produce the same osmotic stress effect on the protein as large osmolytes. Such a universal trend for small and large osmolytes additionally confirms our conclusion about increased hydration of rhodopsin upon light activation.

We also note that high hydrostatic pressure, as well as osmotic stress, shifts the equilibrium of metarhodopsin towards an inactive state [53]. However, their mechanisms of action are completely different. Hydrostatic pressure leads to a change in the molar volume of the protein (i.e., density), but not to a change in the number of water molecules in the receptor. The increase in density may include the penetration of water molecules into small voids or cavities in rhodopsin, void collapse, or alternatively a higher-density solvation shell versus the bulk [54]. On the contrary, in the case of osmotic pressure, there is a change in protein hydration through the (virtual) Gibbs surface, which separates the inner volume of rhodopsin from the outer bulk water. Thus, the two methods complement each other, providing a more complete picture of rhodopsin activation in a hydrated lipid membrane. By analogy with the effect of pressure on protein folding, MI can be considered as more densely packed state in which void volume and solvent amount in internal cavities are minimized, while MII is a less dense state with increased water content in the formed transducin binding cavity.

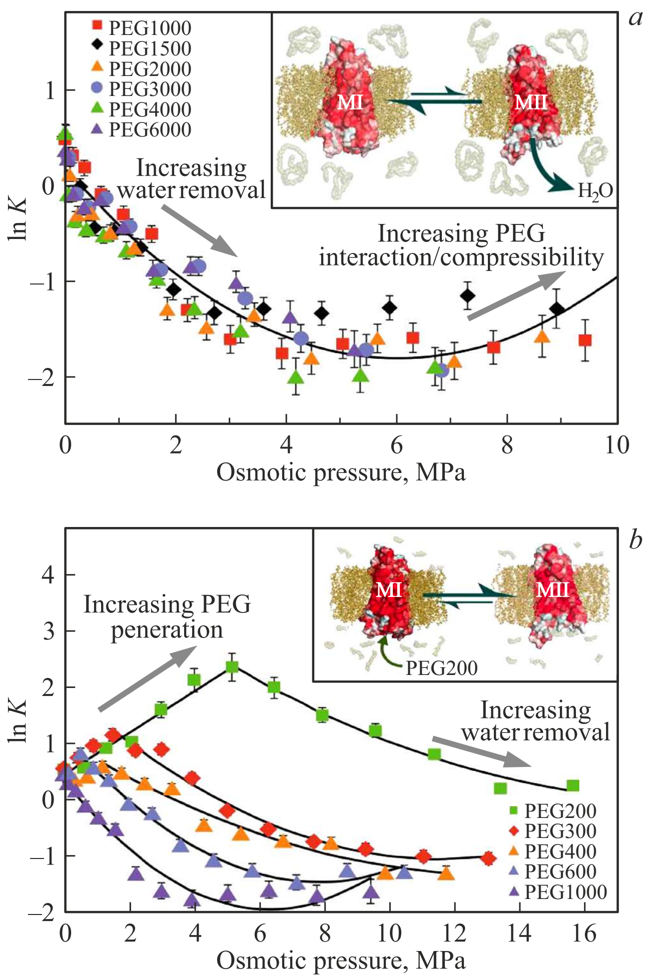

Figure 5. Natural logarithm of the MI–MII equilibrium constant ($K = [\mathrm{MII}]/[\mathrm{MI}]$) demonstrates different behavior on osmotic pressure for (*a*) large and (*b*) small PEGs, yet show a universal trend for excluded polymers at higher concentrations. Inset (*a*) MI–MII equilibrium is shifted to the inactive MI state due to dehydration of rhodopsin by large osmolytes which are completely excluded from the protein. Inset (*b*) Small osmolytes penetrate the G-protein binding site and stabilize the open active MII state. Figure is from Ref. [41].

Still, the question arises: why, at high concentrations of large molecular weight osmolytes, where the effect of compressibility occurs, it leads to a shift to the active state, while hydrostatic pressure shifts the equilibrium towards the inactive state? Here, it should be emphasized that it is difficult to give an unambiguous interpretation to the second virial coefficient appearing in formula (5). If the main contribution to the second term is compressibility, which is associated with fluctuations in the hydration volume of the protein (unlike hydrostatic compressibility of the protein volume), then the sign of the coefficient indicates that the compressibility increases upon transition to the active MII state. That leads to greater volumetric fluctuations that are in good agreement with the model of a hydrated swollen protein in the active state.

Alternatively, the contribution to the second virial coefficient is possibly related to the interactions of osmolytes with the protein, which favor the shift of the equilibrium of metarhodopsin to the active state, for example, interactions with the Glu^{134} hydration center as mentioned above. For large osmolytes at low concentrations, an equilibrium shift to an inactive state is predominant. Yet as the concentration of osmolytes increases, they can penetrate more into the transducin binding cavity in rhodopsin, and the above interactions of osmolytes with the protein can increase. Thus, the combination of a compressibility change and specific interactions of osmolytes with protein can contribute to the second virial coefficient ΔC in the non-linear term of formula (5).

Role of hydration in rhodopsin and transducin activation

The biological relevance of these findings is that water influx into the protein interior enables proton uptake to occur via Glu^{134} of the conserved E(D)RY motif giving the high-hydration, high-affinity $\mathrm{MII}_b\mathrm{H}^+$ substate. Exposure of the G-protein binding cleft allows binding of Gt•GDP by the $\alpha 5$ helix of the transducin C-terminus. However, to ensure the rapid transducin activation rate it cannot remain strongly bound. The G-protein must be released quickly following nucleotide exchange. Here we propose that a hydration-dehydration cycle together with rhodopsin thermal helical fluctuations contributes to a high G-protein binding and unbinding rate. Transducin binding dehydrates the receptor, which leads tio its unbinding and shifting the equilibrium to the inactive MI state. Furthermore, exchange of GTP for GDP yields dissociation of the transducin $\mathrm{G}_{\beta\gamma}$ subunits, dehydrating rhodopsin locally, and withdrawing water in analogy to large polymer osmolytes, giving the partially hydrated MII_b substate. As a result, transducin catalyzes its own release by pinching off the G_α•GTP subunit.

Conclusion

The results in this paper directly show that rhodopsin activation is coupled to large-scale changes in internal protein hydration. They provide clear evidence of an influx of 80–100 water molecules into the protein in the transition from the inactive MI to the active MII state. We describe the opposite effects of large and small osmolytes on the metarhodopsin equilibrium established after photoactivation, where large molar mass solutes that are completely excluded from rhodopsin dehydrate the protein. They back shift the equilibrium to the inactive state, while small osmolytes penetrate the transducin binding cavity and increase the active state fraction. Additionally, it was shown that hydration affects the interaction of the receptor with its cognate G-protein, where the binding affinity of transducin depending on degree of hydration may change by an order of magnitude. These findings suggest a new view of rhodopsin functioning, where water acts as a powerful allosteric modulator of rhodopsin activation and its interaction with effector proteins.

Funding

Work supported by the U.S. National Science Foundation (CHE 1904125 and MCB 1817862) and by the U.S. National Institutes of Health (EY012049 and EY026041) (to M.F.B.). A.V.S. acknowledges partial support from Saint-Petersburg State University (grant 51142660). A.V.S. and A.V.B. were supported by the Russian Foundation for Basic Research (16-04-00494A).

Conflict of interest

The authors declare that they have no conflicts of interest.

References

[1] A.V. Struts, A.V. Barmasov, M.F. Brown. Opt. Spectrosc. **118**, 711 (2015). DOI: 10.1134/S0030400X15050240

[2] A.V. Struts, A.V. Barmasov, M.F. Brown. Opt. Spectrosc. **120**, 286 (2016). DOI: 10.1134/S0030400X16010197

[3] N.R. Latorraca, A.J. Venkatakrishnan, R.O. Dror. Chem. Rev. **117**, 139 (2017). DOI: 10.1021/acs.chemrev.6b00177

[4] D. Hilger, M. Masureel, B.K. Kobilka. Nat. Struct. Mol. Biol. **25**, 4 (2018). DOI:10.1038/s41594-017-0011-7

[5] W.I. Weis, B.K. Kobilka. Annu. Rev. Biochem. **89**, 897 (2018). DOI: 10.1146/annurev-biochem-060614-033910

[6] A.J. Venkatakrishnan, A.K. Ma, R. Fonseca, N.R. Latorraca, B. Kelly, R.M. Betz, ... R.O. Dror. Proc. Natl. Acad. Sci. U.S.A. **116**, 3288 (2019). DOI: 10.1073/pnas.1809251116

[7] H.-W. Choe, Y.J. Kim, J.H. Park, T. Morizumi, E.F. Pai, N. Krauß, . . . O.P. Ernst. Nature **471**, 651 (2011). DOI: 10.1038/nature09789

[8] S.G.F. Rasmussen, H.-J. Choi, J.J. Fung, E. Pardon, P. Casarosa, P.S. Chae, . . . B.K. Kobilka. Nature **469**, 175 (2011). DOI: 10.1038/nature09648

[9] Y. Kang, X.E. Zhou, X. Gao, Y. He, W. Liu, A. Ishchenko, . . . H.E. Xu. Nature **523**, 561 (2015). DOI: 10.1038/nature14656

[10] U.R. Shrestha, S.M.D.C. Perera, D. Bhowmik, U. Chawla, E. Mamontov, M.F. Brown, X.-Q. Chu. J. Phys. Chem. Lett. **7**, 4130 (2016). DOI: 10.1021/acs.jpclett.6b01632

[11] S.M.D.C. Perera, U. Chawla, U.R. Shrestha, D. Bhowmik, A.V. Struts, S. Qian, . . . M.F. Brown. J. Phys. Chem. Lett. **9**, 7064 (2018). DOI: 10.1021/acs.jpclett.8b03048

[12] N. Leioatts, B.M. Mertz, K. Martínez-Mayorga, T.D. Romo, M.C. Pitman, S.E. Feller, ... M.F. Brown, Biochemistry **53**, 376 (2014). DOI: 10.1021/bi4013947

[13] L.A. Salas-Estrada, N. Leioatts, T.D. Romo, A. Grossfield, Biophys. J. **114**, 355 (2018). DOI: 10.1016/j.bpj.2017.11.021

[14] E. Malmerberg, P.H.M. Bovee-Geurts, G. Katona, X. Deupi, D. Arnlund, C. Wickstrand, ... R. Neutze, Sci. Signal. **8**, ra26 (2015). DOI: 10.1126/scisignal.2005646

[15] E. Zaitseva, M.F. Brown, R. Vogel, J. Am. Chem. Soc. **132**, 4815 (2010). DOI: 10.1021/ja910317a

[16] B. Knierim, K.P. Hofmann, O.P. Ernst, W.L. Hubbell, Proc. Natl. Acad. Sci. U.S.A. **104**, 20290 (2007). DOI: 10.1073/pnas.0710393104

[17] M. Mahalingam, K. Martínez-Mayorga, M.F. Brown, R. Vogel, Proc. Natl. Acad. Sci. U.S.A. **105**, 17795 (2008). DOI: 10.1073/pnas.0804541105

[18] C. Altenbach, A.K. Kusnetzow, O.P. Ernst, K.P. Hofmann, W.L. Hubbell, Proc. Natl. Acad. Sci. U.S.A. **105**, 7439 (2008). DOI: 10.1073/pnas.0802515105

[19] O. Soubias, K. Gawrisch, Biochim. Biophys. Acta **1818**, 234 (2012). DOI: 10.1016/j.bbamem.2011.08.034

[20] M.F. Brown, Annu. Rev. Biophys. **46**, 379 (2017). DOI: 10.1146/annurev-biophys-070816-033843

[21] S.D.E. Fried, J.W. Lewis, I. Szundi, K. Martinez-Mayorga, M. Mahalingam, R. Vogel, ... M.F. Brown, Biophys. J. **120**, 440 (2021). DOI: 10.1016/j.bpj.2020.11.007

[22] Z. Salamon, Y. Wang, M.F. Brown, H.A. Macleod, G. Tollin, Biochemistry **33**, 13706 (1994).

[23] Z. Salamon, M.F. Brown, G. Tollin, Trends Biochem. Sci. **24**, 213 (1999).

[24] M.F. Colombo, D.C. Rau, V.A. Parsegian, Science **256**, 655 (1992). DOI: 10.1126/science.1585178

[25] C. Reid, R.P. Rand, Biophys. J. **72**, 1022 (1997). DOI: 10.1016/S0006-3495(97)78754-X

[26] G.D. Dzingeleski, R. Wolfenden, Biochemistry **32**, 9143 (1993). DOI: 10.1021/bi00086a020

[27] J. Zimmerberg, F. Benzanilla, V.A. Parsegian, Biophys. J. **57**, 1049 (1990). DOI: 10.1016/S0006-3495(90)82623-0

[28] I. Vodanoy, S.M. Bezrukov, V.A. Parsegian, Biophys. J. **65**, 2097 (1993). DOI: 10.1016/S0006-3495(93)81245-1

[29] M.D. Rayner, J.G. Starkus, P.C. Ruben, D.A. Alicata, Biophys. J. **61**, 96 (1992). DOI: 10.1016/S0006-3495(92)81819-2

[30] J.A. Kornblatt, G. Hui Bon Hoa, Biochemistry **29**, 9370 (1990). DOI: 10.1021/bi00492a010

[31] J.Y.A. Lehtonen, K.J. Kinnunen, Biophys. J. **66**, 1981 (1994). DOI: 10.1016/s0006-3495(94)80991-9

[32] K.J. Mallikarjunaiah, A. Leftin, J.J. Kinnun, M.J. Justice, A.L. Rogozea, H.I. Petrache, M.F. Brown, Biophys. J. **100**, 98 (2011). DOI: 10.1016/j.bpj.2010.11.010

[33] T.R. Molugu, S. Lee, M.F. Brown, Chem. Rev. **117**, 12087 (2017). DOI: 10.1021/acs.chemrev.6b00619

[34] J.T. McCown, E. Evans, S. Diehl, H.C. Wiles, Biochemistry **20**, 3134 (1981). DOI: 10.1021/bi00514a023

[35] D.C. Mitchell, B.J. Litman, Biochemistry **38**, 7617 (1999). DOI: 10.1021/bi990634m

[36] M. Straume, D.C. Mitchell, J.L. Miller, B.J. Litman, Biochemistry **29**, 9135 (1990). DOI: 10.1021/bi00491a006

[37] V.A. Parsegian, R.P. Rand, D.C. Rau, Meth. Enzymol. **259**, 43 (1995). DOI: 10.1016/0076-6879(95)59039-0

[38] M. Straume, B.J. Litman, Biochemistry **26**, 5113 (1987). DOI: 10.1021/bi00390a033

[39] B.J. Litman, D.C. Mitchell, in Biomembranes, A. Lee, Editor. Vol. 2A. pp. 1–32 (Jai Press, Greenwich, CT, 1996).

[40] U. Chawla, S.M.D.C. Perera, S.D.E. Fried, A.R. Eitel, B. Mertz, N. Weerasinghe, ... M.F. Brown, Angew. Chem. Int. Ed. **60**, 2288 (2021). DOI: 10.1002/anie.202003342

[41] S.D.E. Fried, K.S.K. Hewage, A.R. Eitel, A.V. Struts, N. Weerasinghe, S.M.D.C. Perera, M.F. Brown, Proc. Natl. Acad. Sci. U.S.A. **119**, e2117349119 (2022). DOI: 10.1073/pnas.2117349119

[42] R. Vogel, S. Lüdeke, F. Siebert, T.P. Sakmar, A. Hirshfeld, M. Sheves, Biochemistry **45**, 1640 (2006). DOI: 10.1021/bi052196r

[43] R. Vogel, M. Mahalingam, S. Lüdke, T. Huber, F. Siebert, T.P. Sakmar, J. Mol. Biol. **380**, 648 (2008). DOI: 10.1016/j.jmb.2008.05.022

[44] J. Standfuss, E. Zaitseva, M. Mahalingam, R. Vogel, J. Mol. Biol. **380**, 145 (2008). DOI: 10.1016/j.jmb.2008.04.055
[45] A.V. Botelho, T. Huber, T.P. Sakmar, M.F. Brown, Biophys. J. **91**, 4464 (2006). DOI: 10.1529/biophysj.106.082776
[46] Y. Wang, A.V. Botelho, G.V. Martinez, M.F. Brown, J. Am. Chem. Soc. **124**, 7690 (2002). DOI: 10.1021/ja0200488
[47] C.J. López, M.R. Fleissner, Z. Guo, A.K. Kusnetzow, W.L. Hubbell, Protein Sci. **18**, 1637 (2009). DOI: 10.1002%2Fpro.180
[48] K. Palczewski, T. Kumasaka, T. Hori, C.A. Behnke, H. Motoshima, B.A. Fox, ... M. Miyano, Science **289**, 739 (2000). DOI: 10.1126/science.289.5480.739
[49] T.E. Angel, S. Gupta, B. Jastrzebska, K. Palczewski, M.R. Chance, Proc. Natl. Acad. Sci. U.S.A. **106**, 14367 (2009). DOI: 10.1073/pnas.0901074106
[50] A. Sandoval, S. Eichler, S. Madathil, P.J. Reeves, K. Fahmy, R.A. Böckmann, Biophys. J. **111**, 79 (2016). DOI: 10.1016/j.bpj.2016.06.004
[51] I.A. Shkel, D.B. Knowles, M.T. Record Jr., Biopolymers **103**, 517 (2015). DOI: 10.1002/bip.22662
[52] U. Chawla, S.M.D.C. Perera, A.V. Struts, M.C. Pitman, M.F. Brown, Biophys. J. **110**, 83a (2016). DOI: 10.1016/j.bpj.2015.11.508
[53] A.A. Lamola, T. Yamane, A. Zipp, Biochemistry **13**, 738 (1974). DOI: 10.1021/bi00701a016
[54] D.R. Martin, D.V. Matyushov, J. Phys. Chem. Lett. **6**, 407 (2015). DOI: 10.1021/jz5025433